2,2′-Bis(3-(2-pyridyl)-1-methyltriazolyl)biphenyl: A Tetracoordinating Wrapping Ligand Inducing Similar Skew Coordination Geometries at Copper(I) and Copper(II)

Edgar Müller,*,† Gérald Bernardinelli,‡ and Jan Reedijk†

Leiden Institute of Chemistry, Gorlaeus Laboratories, Leiden University, P.O. Box 9502, 3200 RA Leiden, The Netherlands, and Laboratoire de Cristallographie, University of Geneva, 24 quai Ernest Ansermet, 1211 Genève, Switzerland

Received July 31, 1995[⊗]

The synthesis of a new wrapping ligand, 2,2′-bis(3-(2-pyridyl)-1-methyl-1,2,4-triazol-5-yl)biphenyl (**mbptb**) is described. This ligand induces similar, about 45°-crossed (skew) coordination geometries at both the Cu(I) and the Cu(II) ion. Both $[Cu^{I}(\mathbf{mbptb})]ClO_4$ and $[Cu^{II}(\mathbf{mbptb})](ClO_4)_2$ were characterized by X-ray structure determinations, UV/vis spectroscopy, and electrochemical measurements. The electronic spectrum of the orange Cu(I) complex shows two metal-to-ligand charge transfer bands at 442 and 340 nm, with extinctions ϵ of 1300 and 2600 M^{-1} cm^{-1} respectively, corresponding to excitations into the lowest and the second lowest unoccupied ligand MO. The turquoise Cu(II) compound shows a broad d−d transition with a maximum at 799 nm ($\epsilon = 73.4$ M^{-1} cm^{-1}) with a shoulder at 690 nm, as well as a ligand-to-metal charge transfer transition at 344 nm ($\epsilon = 55$ M^{-1} cm^{-1}). The Cu^{II}/Cu^{I} potential (in acetonitrile) is 0.53 V (NHE).

Introduction

Ligands which induce wrapping type or helical geometries around labile metal ions gain increasingly interest. Highly complex structures may be obtained in some cases through *self-assembling* of simple molecular and ionic components.[1] In a similar approach, a suitable ligand framework may be used to impose an unusual coordination geometry upon a metal ion, e.g. in order to bring it closer to a catalytically active transition state or to tune its redox potential to a desired value. In an earlier paper,[2] some of us described the 2,2′-bis(6-(2,2′-bipyridyl)biphenyl ligand (**TET**), based on a 2,2′-biphenyl spacer unit, which induces a nearly tetrahedral coordination geometry around a Cu(I) ion and thereby strongly stabilizes the copper(I) state. Following the same philosophy, a tighter ligand system was developed which induces an about 45° skew coordination environment. Such an intermediate between the tetrahedral and the square planar geometry is supposed to occur in the *entatic state*[3] of certain copper enzymes which are involved in cellular redox processes. The chemical modeling of such unusual geometries has also been tried by other ways.[4]

Experimental Section

Physical Measurements. ^{1}H- and ^{13}C-NMR spectra were measured on a Bruker ACP-200 equipped with an Aspect 3000 computer; IR spectra were obtained from KBr pills on a Perkin-Elmer PE-580. Mass spectra were obtained on a Finnigan MAT 900 instrument in EI mode with direct insertion probe. Elemental Analyses were carried out by University College, Dublin. Electronic spectra in the UV/vis range were taken in acetonitrile solution on a Perkin-Elmer-330 (copper(I) compound) and on a Perkin-Elmer Lambda-7 (copper(II) compound). A trace of hydrazine was added in the case of the copper(I) compound to prevent oxidation.

Cyclic Voltammograms. These were recorded with a potentiostat controlled by the AMEL 433 software and a conventional 3-electrode configuration, using a glassy carbon working electrode under nitrogen. Tetrabutylammonium hexafluorophosphate (0.1 M in CH_3CN) served as the supporting electrolyte, and the scan speed was 0.2 V/s. The reference electrode was the Ag/Ag^{+} couple, with a potential of 0.592 V (NHE) as standardized against the known potentials of $[Ru(bpy)_3](ClO_4)_2$. The voltammograms were analyzed according to established procedures.[5]

Crystal Structures. Experimental data and structure refinement parameters are given in Table 1. The data for the copper(I) and the copper(II) compounds were collected at ambient temperature on an Enraf Nonius CAD4 and a STOE STADI4 diffractometer respectively, using graphite monochromatized Mo (Kα) radiation. The crystals were mounted in Lindemann capillaries. Data were corrected for polarization and absorption.[6] The structures were solved by direct methods (MULTAN87)[7] and the non-hydrogen atoms were refined anisotropically (XTAL 3.0).[8] Hydrogen atoms were added in calculated positions, except for the non-methyl hydrogens of the copper(II) compound, which were observed and refined with a fixed value of the isotropic displacement parameters.

Ligand Synthesis (Scheme 1). Solvents and Starting Materials. The chemicals used in the syntheses were of commercial grade and

† Leiden University.
‡ University of Geneva.
⊗ Abstract published in *Advance ACS Abstracts,* February 15, 1996.

(1) (a) Lehn, J.-M. In *Perspectives in Coordination Chemistry;* Williams, A. F., Floriani, C., Merbach, A. E., Eds.; Verlag Helvetica Chimica Acta: Basel, Switzerland, and VCH: Weinheim, Germany, 1992; p 447. (b) Baxter, P.; Lehn, J.-M.; DeCian, A.; Fischer, J. *Angew. Chem., Int. Ed. Engl.* **1993**, *32*, 69. (c) Constable, E. C.; Chotalia, R. *J. Chem. Soc., Chem. Commun.* **1992**, 64 and references therein. (d) Constable, E. C.; Ward, M. D. *J. Am. Chem. Soc.* **1990**, *112*, 1256. (e) Piguet, C.; Bünzli, J.-C. G.; Bernardinelli, G.; Hopfgartner, G.; Williams, A. F. *J. Am. Chem. Soc.* **1993**, *115*, 8197. (f) Van Koningsbruggen, P. J.; Müller, E.; Haasnoot, J. G.; Reedijk, J. *Inorg. Chim. Acta* **1993**, *208*, 37. (g) Van Koningsbruggen, P. J.; Van Hal, J. W.; Müller, E.; De Graaff, R. A. G. *J. Chem. Soc., Dalton Trans.* **1993**, 1371.
(2) Müller, E.; Piguet, C.; Bernardinelli, G.; Williams, A. F. *Inorg. Chem.* **1988**, *27*, 849.
(3) (a) Williams, R. J. P.; da Silva, J. R. R. F. *New Trends in Bio-inorganic Chemistry*; Academic Press: London, 1978. (b) Timmons, J. H.; Martin, J. W. L.; Martell, A. E.; Rudolf. P. R.; Clearfield, A. *Inorg. Chem.* **1988**, *27*, 1638.
(4) (a) Yokoi, H.; Addison, A. W. *Inorg. Chem.* **1977**, *16*, 1341. (b) Knapp, S.; Kneenan, T. P.; Zhang, X.; Fikar, R.; Potenza, J. A.; Schugar, H. J. *J. Am. Chem. Soc.* **1987**, *109*, 1882. (c) Garber, T.; Van Wallendael, S.; Rillema, D. P.; Kirk, M.; Hatfield, W. E.; Welch, J. H.; Singh, P. *Inorg. Chem.* **1990**, *29*, 2863.
(5) Bard, A. J.; Faulkner, L. R. *Electrochemical Methods, Fundamentals and Applications*; Wiley; New York; 1980; Chapter 6.
(6) Blanc, E.; Schwarzenbach, D.; Flack, H. D. *J. Appl. Crystallogr.* **1991**, *24*, 1035.
(7) Main, P.; Fiske, S. J.; Hull, S. E.; Lessinger, L.; Germain, G.; Declercq, J.-P.; Woolfson, M. M. *A System of Computer Programs for the Automatic Solution of Crystal Structures from X-Ray Diffraction Data*; Universities of York, England, and Louvain-la-Neuve, Belgium, 1987.
(8) Hall, S. R.; Stewart, J. M., Eds. *XTAL 3.0 Reference Manual*, Lamb: Perth, Australia, 1989.

0020-1669/96/1335-1952$12.00/0

Table 1. Summary of Crystal Data, Intensity Measurement and Structure Refinements for $[Cu^{I}(\mathbf{mbptb})](ClO_4)$ and $[Cu^{II}(\mathbf{mbptb})](ClO_4)_2$

formula	$[Cu(C_{28}H_{22}N_8)]ClO_4 \cdot CH_3CN$	$[Cu(C_{28}H_{22}N_8)](ClO_4)_2 \cdot CH_3CN$
mol wt	674.6	387.0
cryst syst	triclinic	orthorhombic
space group	*P*1	*Cmca*
cell params	from 27 reflcns with $26° < 2\theta < 32°$	from 22 reflcns with $16° < 2\theta < 27°$
a, Å	11.6178(9)	28.571(6)
b, Å	14.9054(12)	16.559(9)
c, Å	19.390(3)	14.077(6)
α, deg	67.793(8)	90
β, deg	81.557(8)	90
γ, deg	78.356(6)	90
V, Å^3	3035.5(6)	6660(5)
Z	4	8
D_{calc}, g cm^{-3}	1.47	1.54
μ, mm^{-1}	0.858	0.881
A^*: min, max	1.206, 1.246	1.109, 1.277
F_{000}	1384	3160
wavelength, Å	0.710 69	0.710 69
no. of unique reflcns	5664 ($4° < 2\theta < 44°$)	2704 ($6° < 2\theta < 48°$)
no. of obsd reflcns	4422 ($\|F_o\| > 4\sigma F_o$)	1492 ($\|F_o\| > 4\sigma F_o$)
no. of params	388	272
weighting scheme	$1/(\sigma F_o)^2$	unit weights
max and av shift/error	0.130, 0.026	0.96, 0.035
max and min diff electr dens, e Å^{-3}	+0.89, −0.73	+0.82, −1.15
R, R_w	0.074, 0.057	0.066, 0.066

Scheme 1. Syntheses of the **bptb** and **mbptb** Ligands

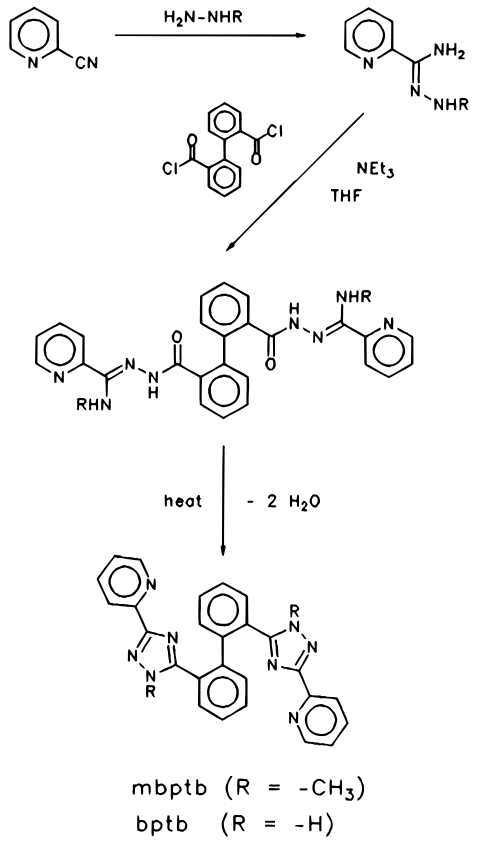

purchased from Fluka, Buchs, Switzerland, and Janssen, Beerse, Belgium. The acetonitrile used in cyclic voltammetry and in UV/vis spectroscopy was distilled over phosphorus pentaoxide.

Crystalline $[Cu^{I}(CH_3CN)_4]ClO_4$ was prepared by reduction of commercial $[Cu^{II}(H_2O)_6](ClO_4)_2$ in acetonitrile with copper powder at 40 °C, filtering, and cooling the resulting colorless solution in ice. *Caution*! Perchlorate salts are potentially explosive and should be handled with the necessary precautions.[9]

Diphenoyl Dichloride. A 24.2 g (0.1 mol) sample of finely powdered diphenic acid was heated under intensive stirring with 50 mL of $SOCl_2$ and 1 mL of dimethylformamide (DMF) as a catalyst at 80 °C for 15−20 min, until the evolution of acid vapors had stopped and the mixture had become entirely homogeneous. Removal of the excessive $SOCl_2$ by distillation gave a residue of crude diphenic acid dichloride, which was distilled *in vacuo* using a short, air-cooled bridge. Gentle heating of the condensation zone with a hot-air gun was necessary to avoid solidification of the product during the distillation. A total yield of 27.0 g (96%) of pure diphenic acid dichloride was collected.

2-Picolyl-*N*-methylamidrazone.[10] A 20.82 g (0.2 mol) sample of 2-cyanopyridine was dissolved in 60 mL of ethanol and 12.0 g (0.26 mol) of methylhydrazine and 3.7 g (0.26 mol) of water were added at once under stirring. The mixture was allowed to stand at room temperature for 3 days, followed by cooling to −20 °C overnight. The crystallized, voluminous bulk of the amidrazone was filtered off, washed with a minimal amount of ethanol, and dried. Yields were typically 60−80%, depending upon conversion. The reaction mixture should not be heated above room temperature; otherwise a dimer, the yellow 1,4-dimethyl-3,6-bis(2-pyridyl)-1,4-dihydro-1,2,4,5-tetrazine, is formed from the amidrazone.

2,2′-Bis(3-(2-pyridyl)-1-methyl-1,2,4-triazol-5-yl)biphenyl (mbptb).[11] To a solution of 3.00 g (20 mmol) of 2-picolyl-N-methylamidrazone and 3.0 g (30 mmol) of triethylamine in 30 mL of tetrahydrofurane (THF) was added a solution of 2.79 g (10 mmol) of diphenoyl dichloride in 10 mL of THF dropwise under vigorous stirring at 0 °C. A white precipitate formed in an exothermic reaction. After completion of the addition, the mixture was warmed up and concentrated to 25 mL. Addition of the same volume of water, followed by filtration of the white precipitate, washing it with water and methanol, and drying it gave the intermediate bis(hydrazide). An intense IR-absorption at 1550−1650 cm^{-1} confirmed the presence of the amide group. *Cyclization* was brought about by heating the dry bis(hydrazide) in a beaker glass on a hot plate to 250 °C (baking method). Under evolution of water vapor, a homogeneous, clear melt was finally obtained, which was dissolved in 15 mL of boiling 2-methoxyethanol to a relatively concentrated solution. Addition of water to this latter solution until the appearance of turbidity and allowing to stand for 3 days yielded the title compound as a white, crystalline product, which was filtered off and dried. Yield: 4.88 g (quantitative).

Anal. Calcd for $C_{28}H_{22}N_8 \cdot H_2O$ (MW 488.551): C, 68.84; H, 4.95; N, 22.94. Found: C, 67.49; H, 4.97; N, 22.18 (two determinations). MS: strongest peak: M^+ cation at *m*/*e* = 470; decay peaks at *m*/*e* 338, 311, 248, and 235. ^{1}H-NMR (in $CDCl_3$; ppm relative to TMS): pyridine signals at 8.640 (2H, ortho to N, pseudodoublet), 7.844 (2H, meta to N, pseudodoublet), 7.615 (2H, para to N, pseudotriplet), 7.210 (2H, meta to N, pseudotriplet); phenyl signals at 7.550 (2H, pseudodoublet), 7.443 (4H, pseudotriplet), 7.286 (2H, pseudodoublet); methyl signal at 3.633 (6H, singlet). A relatively broad peak at 2.852 (2H) indicates a complexed water molecule. ^{13}C-NMR (ppm relative to TMS): 161.96*, 155.34*, 150.00, 149.92*, 140.43*, 137.01, 131.51, 131.46, 130.91, 128.39, 127.31*, 124.01, 121.82, 36.83 (asterisked signals belong to quaternary carbon atoms). IR (cm^{-1}): 3590 m, 3420 s, 3265 m (complexed water); 3050 s (aromatic C−H); 2945 s (−CH_3); 1650 s, 1595 s, 1570 s, 1535 m, 1510 m, 1475 s, 1435 s, 1415 s, 1400 s, 1355 s, 1275 s, 1250 m, 1220 m, 1165 s, 1130 w, 1090 w, 1065 w, 1045 m, 1020 s, 1000 s, 985 m, 965 w, 900 w, 790 s, 780 s, 750 s, 735 s, 705 m, 690 w, 675 s, 660 w, 620 m, 595 w, 545 w, 515 w, 475 w, 430 w, 405 m, 335 w.

(9) Raymond, K. N. *Chem. Eng. News* **1983**, *61* (Dec 5), 4. Wolsey, W. C. *J. Chem. Educ.* **1973**, *50*, A335; *Chem. Eng. News* **1963**, *41* (July 8), 47.

(10) Unsubstituted 2-Picolylamidrazone was obtained in the same way by using 12.0 g of hydrazine hydrate in place of the methylhydrazine and omitting the water.

(11) The unsubstituted **2,2′-Bis-(3-(2-pyridyl)-1,2,4-triazol-5-yl)-biphenyl (bptb)** ligand was obtained in the same way by substituting 2.64 g of 2-picolylamidrazone for the 2−picolyl-N-methylamidrazone. Anal. Calcd for $C_{26}H_{18}N_8$ (MW 442.482): C, 70.58; H, 4.10; N, 25.32. Found: C, 69.81; H, 4.22; N, 23.50. MS: $[M + H]^+$ cation peak at *m*/*e* of 443; strongest peak at *m*/*e* of 297, corresponding to $[M -$ pyridyltriazolyl$]^+$.

Copper Complexes. [Cu^{I}(mbptb)]ClO$_4$·CH$_3$CN.[12] This was obtained by combining equimolar solutions of [Cu(CH$_3$CN)$_4$]ClO$_4$ (327 mg, 1 mmol) and **mbptb** (500 mg, 1.05 mmol) in acetonitrile (5 mL each) under nitrogen. An intense orange color immediately developed, indicating complex formation. The product was precipitated as an orange powder by the addition of ether. Crystals suitable for X-ray diffraction were grown by slow diffusion of ether into a solution of the complex in CH$_3$CN. They tend to lose acetonitrile if stored in air. The compound does not oxidize in the solid state, but acetonitrile solutions of it, upon standing in contact with air for a prolonged time, turned brown due to oxidation of the copper ion. Addition of trace amounts of hydrazine proved to be an efficient mean for keeping the solutions in the reduced state.

Anal. Calcd for $C_{28}H_{22}N_8CuClO_4$·C_2H_3N (MW 674.584): C, 53.42; H, 3.74; N, 18.69; Cu, 9.42. Calcd for $C_{28}H_{22}N_8CuClO_4$ (MW 633.532): C, 53.08; H, 3.50; N, 17.69; Cu, 10.03. Found: C, 51.46; H, 3.66; N, 16.41 (two determinations); Cu, 10.35 (single determination). ^{1}H-NMR (in CD$_3$CN + trace of hydrazine; ppm relative to TMS): 8.466 (2H, pseudodoublet), 8.086 (2H, pseudodoublet), 7.976 (2H, pseudotriplet), 7.42−7.65 (8H, heap of aromatic multiplets), 7.358 (2H, pseudodoublet), 3.928 (6H, singlet). ^{13}C-NMR (ppm relative to TMS): 158.40*, 153.21*, 149.47, 146.28*, 140.62*, 138.48, 131.06, 130.32, 130.00, 128.66, 126.19, 125.54*, 121.12, 36.75 (asterisked signals belong to quaternary carbon atoms).

[Cu^{II}(mbptb)](ClO$_4$)$_2$·CH$_3$CN.[13] This was obtained by mixing equimolar solutions of Cu(ClO$_4$)$_2$·6H$_2$O (0.370 g, 1 mmol) and **mbptb** (500 mg, 1.05 mmol) in acetonitrile (5 mL each). The grass green product precipitated after a short induction period. Crystals suitable for X-ray diffraction were grown by slow evaporation of a saturated solution of the complex in CH$_3$CN.

Anal. Calcd for $C_{28}H_{22}N_8CuCl_2O_8$·C_2H_3N (MW 774.035): C, 46.55; H, 3.26; N, 16.29; Cu, 8.21. Calcd for $C_{28}H_{22}N_8CuCl_2O_8$ (MW 732.983): C, 45.88; H, 3.03; N, 15.29; Cu, 8.67. Found: C, 45.35; H, 3.14; N, 15.45; Cu, 8.57 (single determination).

Results and Discussion

Ligand. The study was first attempted with the unmethylated derivative of the ligand, **bptb**.[6] It became rapidly evident that the chemistry of **bptb** was complicated, due to the ability of the triazole groups to deprotonate and to act as bridging ligands, resulting in low oxidation potentials (autoxidation) in the case of the copper(I) complexes and in polymeric structures (insoluble, difficultly characterizable materials) for the copper(II) compounds. The choice of the bis(1-methyltriazolyl) derivative **mbptb** resolved these problems.[14]

Structure of [Cu^{I}(mbptb)](ClO$_4$)·CH$_3$CN. There are two independent molecules in the asymmetric unit, with similar geometries. The ClO_4^- anions show high displacement parameters, but are not disordered, whereas the CH$_3$CN molecules of crystallization are disordered over two sites. Table 2 gives selected geometrical parameters of the [Cu^{I}(**mbptb**)]$^+$ cation, and Figure 1 shows a drawing of it, with the corresponding atom and ring numbering scheme. The [Cu^{I}(**mbptb**)]$^+$ cation is similar to the [Cu^{I}(**TET**)]$^+$ cation[2] (shown in Figure 3), in the sense that the ligand is wrapped in a **chiral** fashion around the metal center, producing a distorted pseudotetrahedral arrangement of the donor atoms. The "crossing angle" between the two pyridyltriazolyl subunits of the [Cu^{I}(**mbptb**)]$^+$ cation is, however, much smaller (48.9°) than the one observed in the [Cu^{I}(**TET**)] complex (74.9°), situating the present chromophore about midway between a tetrahedral (90°) and a square planar (0°) geometry. Such an environment is likely to be compatible with both, the +I and the +II oxidation state of the copper ion. The local geometry of the CuN$_4$ chromophore is slightly distorted toward a more "tetrahedral" conformation, as indicated by a mean dihedral angle between the (N1,N2,Cu) and the (N5,N8,Cu) planes of 55.1°. The Cu−N bond lengths are comparable with the ones found in the [Cu^{I}(**TET**)]$^+$ cation; the terminal bonds being somewhat longer than the interior ones. The larger values of the dihedral angles, compared to those for

Table 2. Selected Geometrical Parameters of the [Cu^{I}(**mbptb**)]$^+$ Cation (Distances in Å; Angles in deg)

	first molecule	second molecule	mean value[a]	
Cu−N1	2.133(7)	2.132(9)		
Cu−N8	2.016(8)	2.082(8)	Cu−N$_P$	2.091
Cu−N2	1.990(10)	2.050(7)		
Cu−N5	2.068(7)	2.065(10)	Cu−N$_T$	2.043
N1−Cu−N2	81.7(4)	80.7(4)		
N5−Cu−N8	81.5(3)	79.7(4)	N$_P$−Cu−N$_T$	80.9
N1−Cu−N5	141.8(4)	145.9(4)		
N2−Cu−N8	145.4(4)	147.1(4)	N$_P$−Cu−N$_T$′	145.0
N1−Cu−N8	111.7(4)	110.7(4)	N$_P$−Cu−N$_P$	111.2
N2−Cu−N5	108.1(4)	108.6(4)	N$_T$−Cu−N$_T$	108.3
Dihedral Angles between Individual Aromatic Rings				
A−B	1.3	7.5		
E−F	10.4	9.1	pyridyl−triazolyl	7.0
B−C	61.8	67.0		
D−E	66.6	69.2	triazolyl−phenyl	66.2
C−D	71.5	76.3	phenyl−phenyl	73.9
Dihedral Angle between Plane (N1,N2,Cu^{I}) and Plane (N5,N8,Cu^{I})				
	57.1	53.1		55.1
Dihedral Angle between Mean Plane (N1,N2,N3,N4,C1,C2,C3,C4,C5,C6,C7 and Mean Plane (N5,N6,N7,N8,C20,C21,C22,C23,C24,C25,C26) = Pyridyltriazole Chelators				
	52.0	45.8	crossing angle	48.9

[a] Mean values are taken over both halves of both independent molecules; N$_P$ = pyridine nitrogen; N$_T$ = triazole nitrogen.

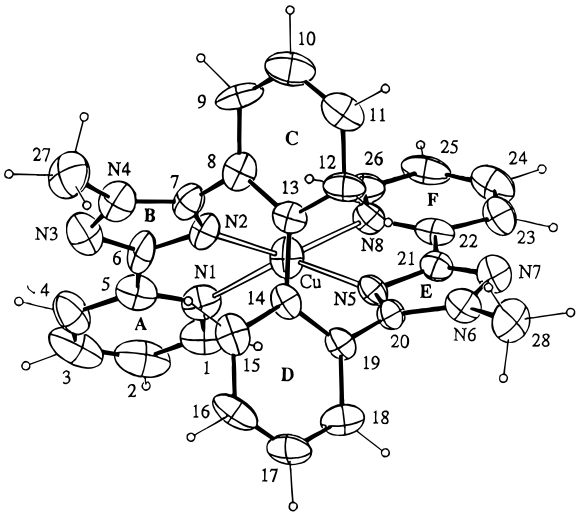

Figure 1. Perspective view of the [Cu^{I}(**mbptb**)]$^+$ cation with atom and ring labeling. Ellipsoids are represented with 35% probability.

(12) The copper(I) complex of the unmethylated ligand, [Cu^{I}(**bptb**)]ClO$_4$, was obtained in the same way from [Cu(CH$_3$CN)$_4$]ClO$_4$ and **bptb** in acetonitrile under nitrogen. An intense orange color immediately developed, indicating complex formation. Addition of ether precipitated the orange complex. It immediately starts to oxidize in contact with air, both in solution and in the solid state, changing its color first to brown and then to green.

(13) The copper(II) complex of the unmethylated ligand, [Cu^{II}(**btpb**)](ClO$_4$)$_2$, was obtained in the same way from Cu(ClO$_4$)$_2$·6H$_2$O and **btpb** in acetonitrile. This complex immediately precipitated upon mixing of the solutions as a grass green, totally insoluble powder.

(14) Although there are two possible, symmetrically methylated derivatives of **btpb**, we focused on the 2,2′-bis(3-(2−pyridyl)-1-methyl-1,2,4-triazol-5-yl)biphenyl ligand. A comparative study of the alternatively possible 2,2′-bis(3-(2-pyridyl)-2-methyl-1,2,4-triazol-5-yl)biphenyl derivative remains for the future.

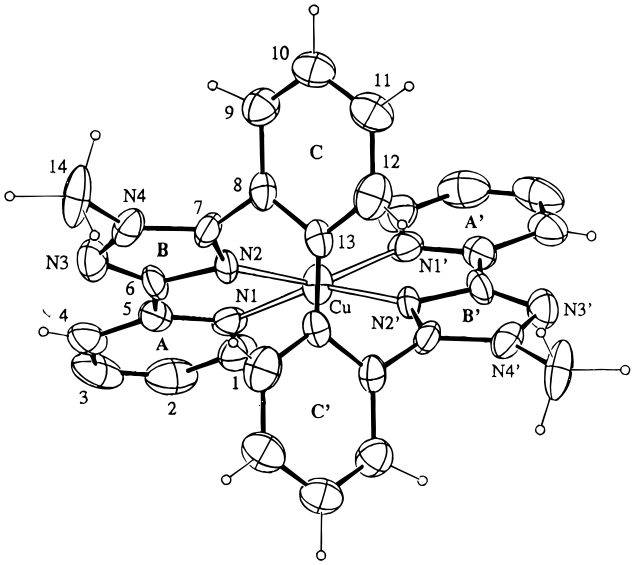

Figure 2. Perspective view of the $[Cu^{II}(\mathbf{mbptb})]^{2+}$ cation along the 2-fold axis with atom and ring labeling. Ellipsoids are represented with 35% probability.

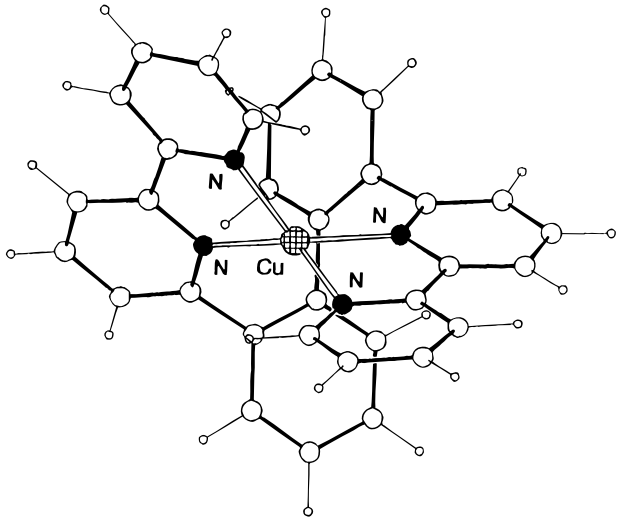

Figure 3. Drawing of the $[Cu^{I}(\mathbf{TET})]^{+}$ cation.[2]

the **TET** complex, between the individual aromatic rings are a mechanical consequence of the flattening of the $[Cu^{I}(\mathbf{mbptb})]$ coordination sphere.

Structure of $[Cu^{II}(mbptb)](ClO_4)_2\cdot CH_3CN$. The asymmetric unit of the crystal consists of half a molecule; the cation lying on a crystallographical 2-fold axis, with copper in special position 8d of the space group *Cmca*. One of the two perchlorate anions is ordered (special position 8e) and the other disordered (special position 8f), as is the solvate acetonitrile molecule. The cation (Figure 2) shows more or less the same geometry as the copper(I) compound. A closer look to the values (Table 3), however, reveals some differences: the coordination environment at the copper(II) ion is flattened by 15° compared to that of the copper(I) complex, as expressed by a dihedral angle of 40.1° between the (N1,N2,Cu) and (N1′,N2′,Cu) planes, in spite of the very similar "crossing angle" of 46.2° between the two pyridyltriazolyl units. The copper(II) ion shows clearly its preference for a square planar coordination environment. Additionally, there are four loose, axial contacts to the oxygen atoms of the ordered perchlorate anion (Cu−O1: 3.011(9) Å; Cu−O2: 3.124(8) Å), resulting in a linear chain throughout the crystal (Figure 7, Supporting Information). Although weak, these "bonds" are strong enough to impede the

Table 3. Selected Geometrical Parameters of the $[Cu^{II}(\mathbf{mbptb})]^{2+}$ Cation (Distances in Å; Angles in deg)[a]

Cu−N1	(Cu−N_P)	2.011(8)
Cu−N2	(Cu−N_T)	1.962(7)
N1−Cu−N2	(N_P−Cu−N_T)	82.0(3)
N1−Cu−N2′	(N_P−Cu−N_T′)	154.0(3)
N1−Cu−N1′	(N_P−Cu−N_P)	103.7(3)
N2−Cu−N2′	(N_T−Cu−N_T)	104.1(3)

Axial Contact Distances with Perchlorate Oxygen Atoms

Cu- -O1	3.011(9)
Cu- -O2	3.124(8)

Dihedral Angles between Individual Aromatic Rings

A−B	6.1	(pyridyl−triazolyl)
B−C	64.5	(triazolyl−phenyl)
C−C′	79.1	(phenyl−phenyl)

Dihedral Angle between Plane (N1,N2,Cu^{II}) and Plane (N1′,N2′,Cu^{II})
40.1

Dihedral Angle between Mean Plane (N1,N2, N3,N4,C1,C2,C3,C4,C5,C6,C7) and Mean Plane (N1′,N2′,N3′,N4′,C1′,C2′,C3′,C4′,C5′,C6′,C7′) = Pyridyltriazole Chelators
46.2 (crossing angle)

[a] N_P = pyridine nitrogen; N_T = triazole nitrogen.

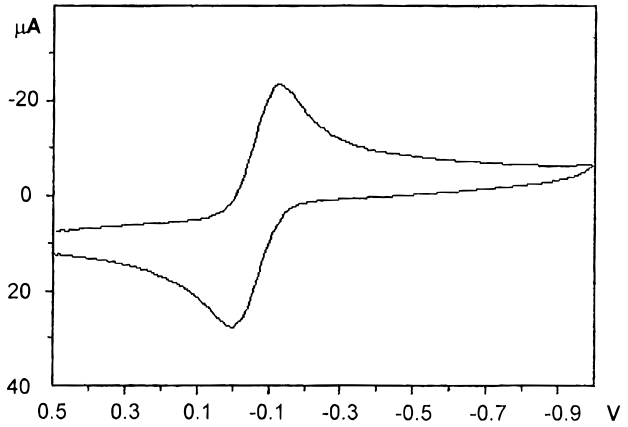

Figure 4. Cyclic voltammogram of $[Cu^{I}(\mathbf{mbptb})](ClO_4)$ in acetonitrile with 0.1 M $(TBA)PF_6$ as supporting electrolyte, a glassy carbon electrode, scan speed of 200 mV/s, and Ag/Ag^{+} reference (potential = 0.592 V (NHE)).

rotation of the perchlorate ion. The Cu−N bond lengths are, as expected, shorter than those of the copper(I) complex; here again, the terminal bonds to the pyridine nitrogen atoms are longer than the interior bonds to the triazole nitrogen atoms.

Electrochemistry. Figure 4 shows a cyclic voltammogram of $[Cu^{I}(\mathbf{mbptb})]ClO_4$ in acetonitrile solution, in the absence of coordinating anions. There is one single, quasi-reversible oxidation−reduction wave at 0.53 V (NHE). This potential is considerably lower than the 0.72 V (NHE) observed under the same conditions for $[Cu^{I}(\mathbf{TET})]ClO_4$;[2] this is a likely consequence of the more planar environment at the copper ion of the $[Cu^{I}(\mathbf{mbptb})]$ chromophore. The amount of out-of-plane rotation of the two diimine chelators has an important effect upon the redox potential of the $Cu^{II/I}$ couple, as seen from the d-orbital correlation diagram in Figure 6: The flatter the environment of the copper ion is, the easier is the removal of an electron from its b_2-orbital.

The potential difference of 132 mV between the oxidation and the reduction peak[15] is more than two times the 56.5 mV

(15) This value is independent of the scan speed, and thus is not due to an ohmic drop in the electrochemical measurement cell.

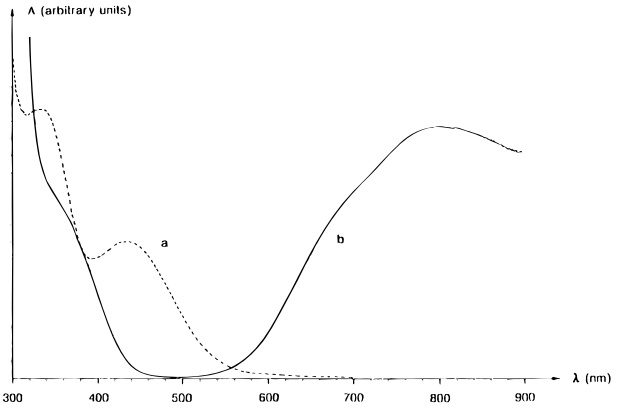

Figure 5. Electronic spectra in acetonitrile: (a) [Cu^{I}(**mbptb**)](ClO_4) ($c = 1.8 \times 10^{-4}$ M) and (b) [Cu^{II}(**mbptb**)](ClO_4)$_2$ ($c = 10^{-2}$ M).

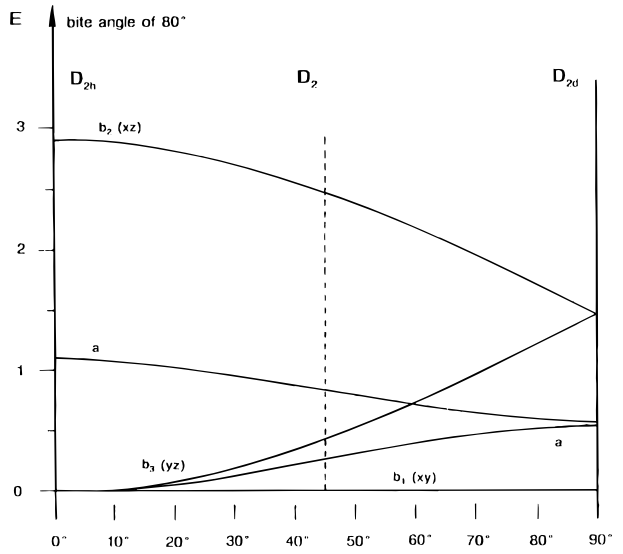

Figure 6. Angular overlap model[23] correlation diagram of the ML_4 $D_{2h} \rightarrow D_{2d}$ distortion pathway (σ-interactions only). Energy in units of M−L interactions.

which would be expected for a perfectly reversible redox process. This indicates that small coordinative rearrangements take place during the oxidation and the reduction step. The observed structural facts (i.e. the flattening of the coordination sphere by 15° and the loose axial coordination of a perchlorate ion in the copper(II) complex) are consistent with these electrochemical finding.

Electronic Spectra. Figure 5 presents the UV/vis spectra of [Cu^{I}(**mbptb**)]ClO_4 and [Cu^{II}(**mbptb**)](ClO_4)$_2$ respectively. The copper(I) compound shows two broad metal-to-ligand charge transfer (MLCT) bands are at 442 nm (crude $\epsilon = 1300$ M^{-1} cm^{-1}) and 340 nm (crude $\epsilon = 2600$ M^{-1} cm^{-1}).[16] Their molar extinctions are lower than those of the [Cu^{I}(**TET**)]$^+$ cation, due to the smaller aromatic acceptor system.[17] The origin of the high energy MLCT band, which is also observed in other Cu^{I}(diimine)$_2$ complexes, remains to be explained.[2]

Hückel calculations show the pyridyltriazole ligand to have a low lying lowest unoccupied molecular orbital (LUMO) of the Orgel Ψ-type,[18] followed by a second lowest unoccupied molecular orbital (SLUMO)[19] 0.6 eV above it and of the Orgel χ-type, as is the highest occupied molecular orbital (HOMO). In this respect pyridyltriazole resembles 2,2′-bipyridine, with the exception that the SLUMO is closer to the LUMO than in bipyridine.

Chart 1. Axes and Characters in D2-Distorted Cu^{I}(**diimine**)$_2$ Complexes

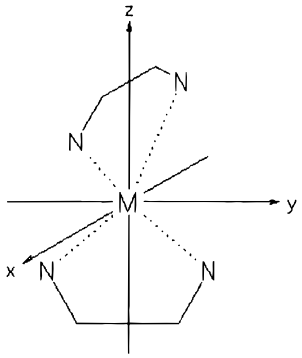

D_2	E	$C_2(z)$	$C_2(y)$	$C_2(x)$	
A	1	1	1	1	x^2, y^2, z^2
B_1	1	1	-1	-1	z xy
B_2	1	-1	1	-1	y xz
B_3	1	-1	-1	1	x yz
4 Lσ	4	0	0	0	$A+B_1+B_2+B_3$
2 Ψ	2	-2	0	0	B_2+B_3
2 X	2	2	0	0	$A+B_1$

Assuming an idealized D_2 symmetry for the [Cu^{I}(mbptb)]$^+$ cation[20] (Chart 1), the two Ψ-ligand-orbitals transform as a b_2 and a b_3 representation, whereas the two χ-ligand-orbitals transform as an a and a b_1 representation. The five copper d-orbitals transform as 2 a (x^2, y^2, z^2), b_1 (xy), b_2 (xz) and b_3 (yz), respectively. Under the given, 45°-crossed, geometry (Figure 6), the b_2 (xz) copper orbital lies about 1.8 eV above the lowest d-orbital (b_1), as seen from the high energy d−d transition of the copper(II) complex, and about 1.2 eV above the next highest d-orbital (a). The b_2 orbital is therefore the only possible donor orbital of the visible MLCT transitions. This allows us to interpret the MLCT absorptions in an unambiguous way: the 442 nm band as a metal-b_2 → LUMO, and the 340 nm band as a metal-b_2 → SLUMO transition, rather than as a consequence of the ligand field splitting at the copper ion. The observed splitting of 6790 cm^{-1} (0.84 eV) between the two MLCT bands, which is significantly smaller than the 8000 cm^{-1} observed in the [Cu^{I}(**TET**)]$^+$ cation,[2] correlates reasonably well with the Hückel predictions of the LUMO−SLUMO gap in pyridyltriazole and pyridine respectively, and not at all with the d−d splitting pattern, which should increase upon flattening of the coordination environment and which has a highest to second highest orbital gap of about 1.2 eV.

The bands can now be assigned as follows: The Cu(I) → LUMO transition transforms as $b_2 \otimes (b_2 + b_3) = a + b_1$ and should be polarized along z (b_1), i.e. the 2-fold axis connecting the two diimine chelators. The Cu(I) → SLUMO transition transforms as $b_2 \otimes (a + b_1) = b_2 + b_3$ and should be polarized along x (b_3) and y (b_2), the remaining two 2-fold axes. There are two allowed transitions into the SLUMO, against a single one into the LUMO, which could explain the reversed intensity

(16) Under the conditions of the experiment ($c = 1.8 \times 10^{-4}$ M in acetonitrile), part of the complex may be dissociated. In the absence of stability information for the [Cu^{I}(mbptb)]$^+$ cation, we estimated its dissociation from the stability constant of the closely related [Cu^{I}(TET)]$^+$ cation in acetonitrile, where a value (log K) of 6.9 was determined.[2] From this, a dissociation of less than 3% is inferred for the present conditions.

(17) Phifer, C. C.; McMillin, D. R. *Inorg. Chem.* **1986**, *25*, 1329.

(18) Orgel, L. E. *J. Chem. Soc.* **1961**, 3683.

(19) Kaim, W.; Ernst, S. *J. Am. Chem. Soc.* **1986**, *108*, 3578.

(20) Atkins, P. W.; Child, M. S.; Phillips, C. S. G. *Tables for Group Theory*, Oxford University Press: Oxford, England, 1970.

ratio of the MLCT absorptions, compared to the one observed for the $[Cu^{I}(\mathbf{TET})]^{+}$ cation.[2]

The spectrum of the $[Cu^{II}(\mathbf{mbptb})](ClO_4)_2$ shows a complex pattern of d−d transitions at the lower energy end, with a prominent feature at 799 nm ($\epsilon = 73.4\ M^{-1}\ cm^{-1}$) preceded by a shoulder at 690 nm, as well as a ligand-to-metal charge transfer (LMCT) transition at 344 nm ($\epsilon = 55\ M^{-1}\ cm^{-1}$). At higher energies, the spectrum is dominated by ligand $\pi-\pi^*$ transitions. The d−d splitting amounts therefore to about 1.8 eV (for the $b_1 \rightarrow b_2$ transition, Figure 6), with the next orbital(s) (a, b_3) about 1980 cm^{-1} (0.25 eV) above the b_1-orbital. The LMCT corresponds to an allowed nitrogen lone pairs ($a + b_1 + b_2 + b_3$) → Cu (b_2) transition.

Conclusions

Distorted "tetrahedral" copper complexes are model compounds for the redox-active Type I copper centers of certain metalloproteins.[21] The dependency of the copper redox potential on the dihedral (twist) angle of the chelators has already been demonstrated for a CuN_2S_2 chromophore.[22] The present study shows that the same holds as well in the case of a CuN_4 chromophore. Sulfur atoms in the coordination sphere of the copper ion are thus known to be nonessential in producing a high redox potential; the more important factor in this respect is the geometry of the ligand environment.

The electronic spectrum of the $[Cu^{I}(\mathbf{mbptb})]^{+}$ cation permitted an unambiguous assignment of the metal-to-ligand charge transfer absorption bands: the first MLCT band corresponds to a Cu(b_2) → LUMO, and the second, higher energy MLCT band to a Cu(b_2) → SLUMO transition. The d−d spectrum of the $[Cu^{II}(\mathbf{mbptb})]^{2+}$ cation is in accord with the angular overlap model[23] predictions (Figure 6) for this particular coordination geometry.

The lower potential (0.53 V) of $[Cu^{I}(\mathbf{mbptb})]^{+}$, compared to the 0.72 V of the earlier described $[Cu^{I}(\mathbf{TET})]^{+}$ cation,[2] allows its reaction with molecular oxygen. At the same time, the copper ion remains accessible for weak coordination with additional ligands at the axial sites. Such complexes might, in consequence, be useful as oxygenation catalysts for organic substrates. The high oxidation resistance, as well as the general chemical inertness of the present, pyridotriazole based ligand framework are favorable factors in this context. The [Cu(**mbptb**)] complexes are finally, ***C*$_2$-symmetric, intrinsically chiral compounds**.[24] Although the ligand might racemize via a partial decomplexation and rotation through its backbone, suitable modifications of this latter, e.g. substitution with bulky groups or use of binaphtyl derivatives, will lead to nonracemizable derivatives for application in chiral homogeneous catalysis.

Acknowledgment. E.M. thanks the Schweizerischer Nationalfonds for a 2-year grant, allowing him to conduct, among others, most of this research at Leiden University, Leiden, The Netherlands. We are further indepted to Dr. J. G. Haasnoot, Mr. G. A. van Albada, and R. A. M. van der Hoeven (Leiden Institute of Chemistry) for assistance with the analyses of ligands and complexes. Prof. A. Williams (University of Geneva) is acknowledged for valuable discussion, as well as Dr. D. Jacoby (University of Lausanne) for the growth of a single crystal.

Supporting Information Available: Tables of atomic coordinates, displacement parameters, bond distances, and bond angles, and dihedral angles and packing diagrams for $[Cu^{I}(\mathbf{mbptb})](ClO_4)\cdot CH_3CN$ and $[Cu^{II}(\mathbf{mbptb})](ClO_4)_2\cdot CH_3CN$, particular views and stereodrawings of the $[Cu^{I}(\mathbf{mbptb})]^{+}$ and the $[Cu^{II}(\mathbf{mbptb})]^{2+}$ cations, a comparative table of Hückel results for the pyridyltriazole and the bipyridyl residue, and Figure 7, the axial contacts of $[Cu^{II}(\mathbf{mbptb})]^{2+}$ with one of the perchlorate anions (16 pages). Ordering information is given on any current masthead page.

IC950983E

(21) Addison, A. W. *Spectroscopic and Redox Trends From Model Copper Complexes*, in *Copper Coordination Chemistry: Biochemical & Inorganic Perspectives*; Karlin, K. D., Zubieta, J., Eds.; Adenine Press: New York, 1983.

(22) Dorfman, J. R.; Bereman, R. D.; Whangbo, M.-H. Utilization of Pseudo-Tetrahedral Copper(II) Coordination Compounds to Interpret the Stereoelectronic Properties of Type I Copper(II) centers in Metalloproteins. In *Copper Coordination Chemistry: Biochemical & Inorganic Perspectives*; Karlin, K. D., Zubieta, J., Eds.; Adenine Press: New York, 1983.

(23) Schäffer, C. E. *Struct. Bonding* **1968**, *5*, 68.

(24) Whitesell, J. K. C_2 Symmetry and Asymmetric Induction. *Chem. Rev.* **1989**, *89*, 1581.